Inorganica Chimica Acta 423 (2014) 36–45

Contents lists available at ScienceDirect

Inorganica Chimica Acta

journal homepage: www.elsevier.com/locate/ica

Structural, magnetic and theoretical study of mononuclear nickel(II) and cobalt(II) compounds of a benzimidazole thiobutanoic acid derivative

Francisco Yoe [a], Marcos Flores-Alamo [a], Francisco Morales [b], Roberto Escudero [b],*, Héctor Cortes-Hernández [c], Miguel Castro [c], Norah Barba-Behrens [a],*

[a] Departamento de Química Inorgánica, Facultad de Química, Universidad Nacional Autónoma de México, México D.F. 04510, Mexico
[b] Instituto de Investigaciones en Materiales, Universidad Nacional Autónoma de México, México D.F. 04510, Mexico
[c] Departamento de Física y Química Teórica, Facultad de Química, Universidad Nacional Autónoma de México, México D.F. 04510, Mexico

ARTICLE INFO

Article history:
Received 8 March 2014
Received in revised form 3 July 2014
Accepted 9 July 2014
Available online 25 July 2014

Keywords:
4-(Benzimidazol-2-yl)-3-thiabutanoic acid
Co^{2+} and Ni^{2+} compounds
Antiferromagnetic behavior
Non-covalent interactions

ABSTRACT

A structural, magnetic and theoretical study of the mononuclear octahedral cobalt(II) and nickel(II) coordination compounds with the tridentate ligand, 4-(benzimidazol-2-yl)-3-thiabutanoic acid (Hbztb), was performed. At low temperature, both compounds present weak antiferromagnetic couplings via intermolecular interactions. In the $[Co(bztb)_2]\cdot H_2O$ compound, intermolecular hydrogen bonding between the benzimidazolic nitrogen atom and the neighboring carboxylic oxygen contribute to the magnetic pathway for the coupling between the cobalt(II) mononuclear complexes. Whereas in $[Ni(bztb)_2]\cdot 3H_2O$, two nickel(II) compounds are linked by non-covalent interactions through water molecules, $[(Ni(bztb)_2\cdots(H_2O)_3\cdots Ni(bztb)_2]$, which play an important role on the super-exchange magnetic coupling contributing to the magnetic MO. The magnetic behavior of both coordination compounds was analyzed by DFT theoretical calculations.

© 2014 Elsevier B.V. All rights reserved.

1. Introduction

In recent years, it has been a considerable interest on supramolecular self-assembly of coordination polymers, where the construction of molecular networks based on organic ligands and metal ions has been a useful approach. These systems have potential utility as molecular-based magnetic materials, induced by metal–metal interactions [1–3], through bridging ligands [4–7] or intermolecular non-covalent interactions such as hydrogen bonding and π–π stacking [1,8,9].

Recently it has been shown that mono-, bis- or tris-chelate mononuclear transition metal coordination compounds may present magnetic interactions, ferromagnetic [10–13] or antiferromagnetic [14–18]. In all cases, this magnetic behavior is due to non-covalent intermolecular forces [18–23].

Benzazoles and their derivatives are an important class of compounds that occur widely as biologically active natural products, their derivatives may present biocide, or antineoplastic properties [24–30]. Among these derivatives there are several examples of 2-substituted benzimidazoles that stabilize a free radical, such as 2-(N-tert-butylaminoxyl)-benzimidazole [31,32], 2-nitronyl nitroxide benzimidazole [10] and 2-mercaptobenzimidazole [33].

The presence of N, S, O atoms in tridentate ligands is highly relevant when interacting with transition metal ions, stabilizing different coordination numbers and geometries [34–37]. Some of these ligands may be regarded as mimics of amino acid side chains, which are involved in coordination to metal ions in proteins and metalloenzymes [38,39]. These tridentate model compounds have shown to mimic metalloenzyme catalytic activities [39,40], or they may interact with DNA fractions [41–43]. Additionally, these coordination compounds may present catalytic activity [44,45] or photoluminescent properties [46,47].

The 4-(benzimidazol-2-yl)-3-thiabutanoic acid (Hbztb), Scheme 1, is a tridentate ligand bearing N, O and S donor atoms [48], where the sulfur is a stereogenic atom, that upon coordination to a metal ion adopts a *S* or *R* conformation. This ligand may stabilize different octahedral geometrical isomers, *fac* or *mer*, with a *cis-cis-cis* or *cis-cis–trans* arrangements [49]. We were interested to investigate the magnetic properties of mononuclear coordination compounds of cobalt(II) and nickel(II) with this versatile ligand, which may contribute to the understanding of non-covalent interactions into their magnetic properties. Herein we report the synthesis, structural characterization and magnetic properties of the obtained com-

---

* Corresponding author. Tel./fax: +52 (55)5622 3810.
E-mail address: norah@unam.mx (N. Barba-Behrens).

http://dx.doi.org/10.1016/j.ica.2014.07.025
0020-1693/© 2014 Elsevier B.V. All rights reserved.

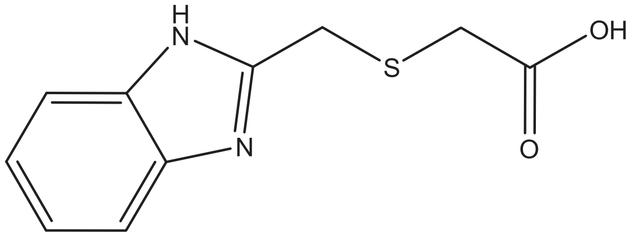

Scheme 1. Structure of 4-(benzimidazol-2-yl)-3-thiabutanoic acid (Hbztb).

pounds. DFT calculations were performed to analyze the contribution of non-covalent interactions on their magnetic couplings.

2. Experimental

2.1. Physical measurements

IR spectra in the range 4000–400 cm^{-1} were recorded in a Perkin Elmer FT-IR Spectrum 400 spectrophotometer with a universal ATR sampling accessory at 298 K. Electronic spectra of powdered crystalline samples were measured, over the range 40000–5000 cm^{-1}, by the diffuse reflectance method on a Cary-5000 Varian spectrophotometer at 298 K. Elemental analyses were carried out with a Fisons EA 1108 analyzer. Magnetic susceptibility measurements at RT of powdered samples were recorded on a Johnson–Matthey DG8 5HJ balance, using the Gouy method. Variable-temperature magnetic susceptibility data for **1** and **2** were collected using a Quantum Design MPMS SQUID magnetometer equipped with 5 T magnet, in a range of 2–300 K. EPR spectra were recorded on polycrystalline samples with a Bruker Elexsys E500 spectrometer using the X-band (9.45 GHz) microwave frequency operating at 100 kHz.

2.2. Materials

The metal salts $[Co(O_2CMe)_2(H_2O)_2]\cdot 2H_2O$, $[Co(NO_3)_2(H_2O)_4]\cdot 2H_2O$, $[Ni(O_2CMe)_2(H_2O)_2]\cdot 2H_2O$, $[Ni(NO_3)_2(H_2O)_4]\cdot 2H_2O$ and 4-(benzimidazol-2-yl)-3-thiabutanoic acid (Aldrich Chem) and methanol (J.T. Baker) were used without further purification.

2.3. Synthesis

The same compounds were obtained regardless of the metal salt used in the synthesis, acetate or nitrate. The synthesis of the coordination compounds, when using the acetate salts, is described below.

2.3.1. Synthesis of compound $[Co(bztb)_2]\cdot 2H_2O$ (**1**)

Cobalt(II) acetate trihydrate (0.0119 g, 0.05 mmol) was dissolved in methanol (1 mL) and added to solution of 4-(benzimidazol-2-yl)-3-thiabutanoic acid (Hbztb) (0.0222 g, 0.1 mmol) in methanol (4 mL). A dark pink solution was refluxed for 2 h and the solution was allowed to stand at low temperature for 3 weeks. The resulting dark pink crystals were suitable for X-ray diffraction analysis. (Yield 0.025 g, 73%). *Anal.* Found: C, 46.16; H, 3.55; N, 10.83%. Calc. for $C_{20}H_{22}N_4O_6S_2Co$: C, 46.24%; H, 3.88%; N, 10.79%. IR, $\nu(cm^{-1})$: ν(C=C) 1627, ν(C=N) 1605, ν(C–N) 1278, $\nu_{as}(COO^-)$ 1575, $\nu_s(COO^-)$ 1381; UV–Vis–NIR, $\nu(cm^{-1})$: $\nu_1 = 8250$, $\nu_2 = 16500$, $\nu_3 = 20450$. RT $\mu_{eff} = 6.48$ BM/Co^{2+}.

2.3.2. Synthesis of compound $[Ni(bztb)_2]\cdot 3H_2O$ (**2**)

In a similar procedure to that described above, addition of Hbztb (0.0222 g, 0.1 mmol) to $Ni(O_2CMe)_2\cdot 3H_2O$ (0.0124 g, 0.05 mmol) gave a light green solution. It was allowed to stand at low temperature for three weeks. Pale green crystals suitable for X-ray diffraction analysis were isolated. (Yield: 0.0181 g, 53%). *Anal.* Found: C, 43.76; H, 4.46; N, 10.04%, Calc. for $C_{20}H_{24}N_4O_7S_2Ni$: C, 43.31; H, 4.36; N, 10.10%. IR, $\nu(cm^{-1})$: ν(C=C) 1632, ν(C=N) 1603, ν(C–N) 1277, $\nu_{as}(COO^-)$ 1583, $\nu_s(COO^-)$ 1367; UV–Vis–NIR, $\nu(cm^{-1})$: $\nu_1 = 9300$, $\nu_2 = 15500$, $\nu_3 = 25000$: RT $\mu_{eff} = 4.69$ BM/Ni^{2+}.

2.4. X-ray crystallographic study

The crystals of **1** and **2** were mounted on glass fiber and studied with a Oxford Diffraction Gemini "A" diffractometer with a CCD area detector, with radiation source of $\lambda_{Mo\ K\alpha} = 0.71073$ Å using graphite-monochromatized radiation. CrysAlis Pro and CrysAlis RED software packages [50] were used for data collection and data integration. A data sets consisted of frames of intensity data collected with a frame width of 1° in ω, a counting time of 1.7–6.8 s/frame, and a crystal-to-detector distance of 55.00 mm. The double pass method of scanning was used to exclude any noise. The collected frames were integrated by using an orientation matrix determined from the narrow frame scans. Final cell constants were determined by a global refinement; collected data were corrected for absorbance by using analytical numeric absorption correction [51] using a multifaceted crystal model based on expressions upon the Laue symmetry using equivalent reflections.

Structure solution and refinement were carried out with the program(s): SHELXS97 [52], SHELXL97; for molecular graphics: ORTEP-3 for Windows [53] and the software used to prepare material for publication: WinGX 1.80.05 [54,55].

Full-matrix least-squares refinement was carried out by minimizing $(F_o^2 - F_c^2)^2$. All non-hydrogen atoms were refined anisotropically. For **1** the H atoms of the water group (H–O) and amine group (H–N) were located in a difference map and refined isotropically with $U_{iso}(H) = 1.5$ and 1.2 U_{eq} for (O) and (N) respectively, while

Table 1
Crystal data and structure refinement for **1** and **2**.

Empirical formula	$C_{20}H_{22}N_4O_6S_2Co$	$C_{20}H_{24}N_4O_7S_2Ni$
Formula weight	537.47	555.26
Color, habit	pink lamina	green plate
Crystal size (mm)	0.51 × 26 × 0.11	0.30 × 0.20 × 0.12
Crystal system	monoclinic	hexagonal
Space group	$P2_1/n$	$P3_1$
Unit cell dimensions		
a (Å)	9.3674(6)	13.78485(4)
b (Å)	13.3630(8)	13.7848(4)
c (Å)	9.7109(7)	10.2753(3)
α (°)	90	90
β (°)	116.19(9)	90
γ (°)	90	120
V (Å^3)	1090.73(12)	1690.93(9)
Z	2	3
Absorption coefficient (mm^{-1})	1.025	1.097
2θ range (°)	3.84–26.05	3.41–26.05
D_{calc} (Mg/m3)	1.636	1.636
Temperature (K)	298 (2)	130 (2)
Reflections collected	7805	12 427
Independent reflections (R_{int})	2156 (3.17%)	4376 (3.57%)
R indices [$I > 2\sigma(I)$] (%)	$R_1 = 0.0293$, $wR_2 = 0.067$	$R_1 = 0.0541$, $wR_2 = 0.135$
R indices [all data] (%)	$R_1 = 0.0381$, $wR_2 = 0.073$	$R_1 = 0.0641$, $wR_2 = 0.142$
Goodness-of-fit (GOF) on F^2, S	1.054	1.017
Data-to-parameters ratio	2156/0/160	4376/51/332

Symmetry operation for compound **1**: x, y, z; 1/2 – x, 1/2 + y, 1/2 – z; –x, –y, –z; 1/2 + x, 1/2 – y, 1/2 + z.
Symmetry operation for compound **2**: x, y, z; –y, x – y, 1/3 + z; –x + y, –x, 2/3 + z.

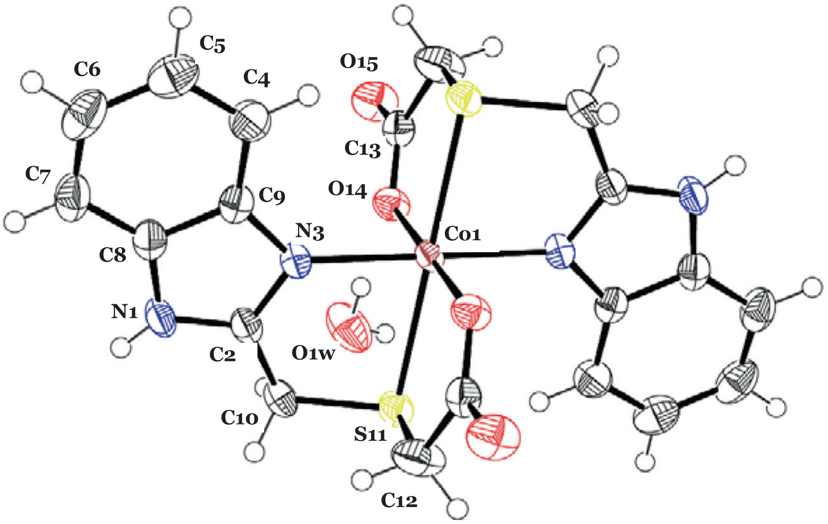

Fig. 1. ORTEP diagram of compound $[Co(bztb)_2]\cdot 2H_2O$ 1. (Displacement ellipsoids are drawn at 30% probability).

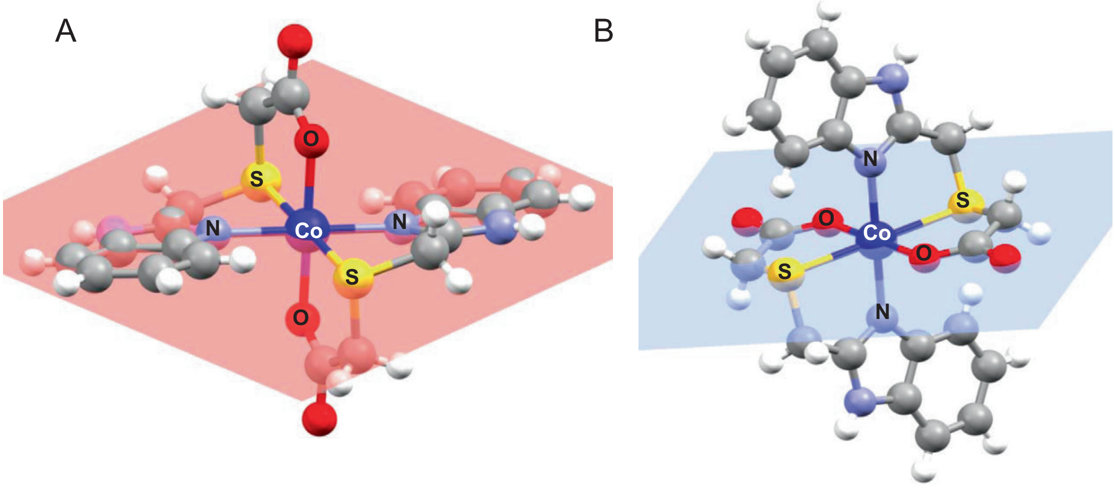

Fig. 2. $[Co(bztb)_2]\cdot H_2O$: (A) plane N3, S11, N3a, S11a; (B) plane O14, S11, O14a, S11a.

Table 2
Selected bond lengths (Å) and angles (°) for the cobalt(II) **1** and nickel(II) **2** compounds.

Co(1)–N(3)	2.123(16) Å	N(3)–Co (1)–S(11)	80.82(5)°		
Co(1)–S(11)	2.493(5) Å	N(3)–Co(1)–O(14)	90.48(6)°		
Co(1)–O(14)	2.054(13) Å	O(14)–Co(1)–S(11)	97.40(4)°		
Ni(1)–N(23)	2.064(7) Å	Ni(1)–N(3)	2.099(7) Å		
S(11)–Ni(1)	2.417(2) Å	S(31)–Ni(1)	2.425(2) Å		
O(14)–Ni(1)	2.002(5) Å	O(34)–Ni(1)	2.019(6) Å		
N(23)–Ni(1)–N(3)	172.1(3)°	S(11)–Ni(1)–S(31)	95.46(8)°	O(14)–Ni(1)–O(34)	94.6(2)°
N(23)–Ni(1)–S(11)	92.9(2)°	O(14)–Ni(1)–S(11)	85.54(19)°	O(14)–Ni(1)–N(23)	95.6(3)°
N(3)–Ni(1)–S(11)	82.63(18)°	O(34)–Ni(1)–S(11)	177.03(19)°	O(34)–Ni(1)–N(23)	90.0(3)°
N(23)–Ni(1)–S(31)	83.75(19)°	O(14)–Ni(1)–S(31)	178.8(2)°	O(14)–Ni(1)–N(3)	90.5(3)°
N(3)–Ni(1)–S(31)	90.2(2)°	O(34)–Ni(1)–S(31)	84.41(17)°	O(34)–Ni(1)–N(3)	94.4(2)°

for **2** the H atoms of the water group (H–O) and amine group (H–N) were located in a difference map and refined as riding on their parent atoms with $U_{iso}(H) = 1.5$ and $1.2\ U_{eq}$ for (O) and (N) respectively. H atoms attached to C atoms were placed in geometrically idealized positions and refined as riding on their parent atoms, with C–H = 0.93–0.99 Å and with $U_{iso}(H) = 1.2\ U_{eq}(C)$ for aromatic and methylene groups. The crystal **2** studied was a racemic twin; the minor twin component refined to 26(3)%. Crystal data and experimental details of the structures determination are listed in Table 1.

3. Results and discussion

3.1. Spectroscopic characterization

The diffuse reflectance spectrum of $[Co(bztb)_2]\cdot 2H_2O$ **1**, presented bands characteristic of an octahedral geometry for cobalt(II), $\nu_1\,{}^4T_{2g}(F) \leftarrow {}^4T_{1g}(F)$, at 8250 cm^{-1}; $\nu_2\,{}^4A_{2g}(F) \leftarrow {}^4T_{1g}(F)$ at 16500 cm^{-1} and $\nu_3\,{}^4T_{1g}(P) \leftarrow {}^4T_{1g}(F)$ at 20450 cm^{-1}. Compound $[Ni(bztb)_2]\cdot 3H_2O$ **2**, showed transitions at 9300, 15500 and

Table 3
Hydrogen bonds for **1** and **2** [(Å) and (°)].

D–H···A	d(D–H)	d(H···A)	d(D···A)	<(DHA)
$[Co(bztb)_2]\cdot 2H_2O$				
O(1W)–H(1W)···O(14)#2	0.83(3)	1.97(3)	2.787(2)	168(3)
N(1)–H(1N)···O(15)#3	0.80(2)	2.16(3)	2.943(2)	168(2)
O(1W)–H(2W)···O(15)#4	0.84(3)	2.04(3)	2.862(3)	168(3)
$[Ni(bztb)_2]\cdot 3H_2O$				
N(21)–H(1)···O(3W)#1	0.93(2)	2.03(3)	2.935(14)	164(1)
N(1)–H(1)···O(1W)#1	0.94(11)	1.86(11)	2.738(3)	158(1)
O(1W)–H(1)···O(15)#2	0.66	1.80(2)	2.706(2)	164(1)
O(2W)–H(2)···O(35)#3	0.91	1.85(1)	2.741(2)	164(1)
O(3W)–H(2)···O(34)#3	0.83	2.07(8)	2.879(2)	166(1)
O(2W)–H(2E)···O(3W)#4	0.94	1.81(2)	2.729(3)	170(1)
O(3W)–H(3E)···O(15)#5	0.85	2.27(1)	3.033(2)	149(1)
N(1)–H(2)···O(2W)#6	0.94(11)	2.10(10)	2.781(13)	130(1)

D = donor, A = acceptor.
Symmetry transformations used to generate equivalent atoms for **1**: #1 $-x, -y+1, -z$ #2 x, y, z #3 $-x-1/2, y-1/2, -z+1/2$ #4 $x-1/2, -y+3/2, z-1/2$.
Symmetry transformations used to generate equivalent atoms for **2**: #1 x, y, z; #2 $-x+y+1, -x+1, z+2/3$; #3 $-x+y, -x+1, z+2/3$; #4 $-y+1, x-y+1, z+1/3$; #5 $-y, x-y, z+1/3$; #6 $-x+y+1, -x+1, z-1/3$.

25000 cm^{-1}, assigned to ν_1 $^3T_{2g}(F) \leftarrow {}^3A_{2g}(F)$, ν_2 $^3T_{1g}(F) \leftarrow {}^3A_{2g}(F)$, and ν_3 $^3T_{1g}(P) \leftarrow {}^3A_{2g}(F)$, for a nickel(II) in an octahedral geometry.

3.2. X-ray diffraction analysis

There are only three reported X-ray crystal structures of coordination compounds with bztb, $[Re(bztb)(CO)_3]$ [35], $[Ni(bztb)_2]\cdot 3EtOH$ and $[Cu(bztb)_2]\cdot 2H_2O$ [49]. All of them are mononuclear compounds, where the deprotonated bztb behaves as a tridentate ligand giving place to *fac*-octahedral geometries. The $[Ni(bztb)_2]\cdot 3EtOH$ and $[Cu(bztb)_2]\cdot 2H_2O$ compounds crystallized in a monoclinic system (P_{21}/n). Nevertheless, they stabilized different isomers, being the nickel(II) compound an all-*cis* isomer, while in the copper(II) compound the sulfur atoms are *trans*- to each other. The complexes obtained in this work present different isomers to both compounds, as will be discussed.

3.2.1. Compound $[Co(bztb)_2]\cdot 2H_2O$ **1**

Compound **1** consists of two deprotonated 4-(benzimidazol-2-yl)-3-thiabutanoic ligands (bztb), tricoordinated to the metal center. The cobalt(II) ion stabilizes a *fac*-octahedral geometry, with the bztb donor atoms in an all-*trans* arrangement, which can be described as *fac*-all *trans*, Fig.1.

Two nitrogen and two sulfur atoms are in an equatorial square planar arrangement around the cobalt(II), the plane N3, S11, N3a, S11a shows a slight distortion of 0.0168 Å, Fig. 2A. Deviations from the orthogonality are shown by the distances Co1–N3 2.123(1), Co1–S11 2.493(1) Å, and bond angles N3–Co1–S11 of 80.82(5), N3–Co1–S11a 99.18(5)° (Table 2). Coordination of the oxygen and sulfur atoms form chelate angles of O14–Co1–S11, 82.60(4) and O14–Co1–S11a, 97.40(4)°, with the oxygen and sulfur atoms (O14, S11, O14a, S11a) forming a fairly regular square planar plane, with a deviation of only 0.0036 Å, Fig. 2B. The distance Co–O 2.055(1) Å, is in the expected range for a Co–O bond length in similar tridentate compounds (Co–O 2.065(6) Å) [56].

It is observed an intermolecular hydrogen bonding between the proton of the benzimidazole nitrogen atom with the oxygen atom from a neighboring carboxylate group (N3–H···O15), with an angle of 168° and a distance D···A of 2.16 Å, which may be considered as a strong interaction. The water molecule present hydrogen bonds with two adjacent carboxylate oxygen atoms, O1w–H2w···O15a and O1w–H1w···O14, with symmetry operations *x*, *y*, *z* and $x-1/2$, $-y+3/2$, $z-1/2$ respectively (Table 3, Fig. 3), providing complex tridimensional interactions in a supramolecular array

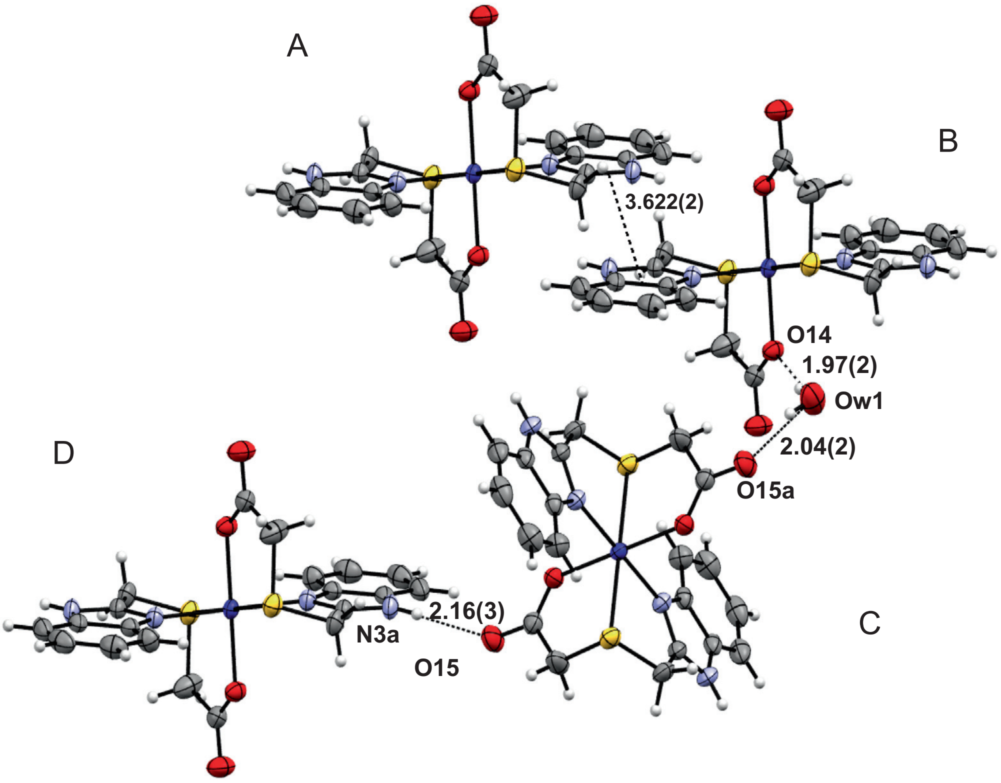

Fig. 3. Intermolecular interactions (Å), in $[Co(bztb)_2]\cdot 2H_2O$: π-stacking of the aromatic rings; hydrogen bonding between N3–H···O15–C13; hydrogen bonding of two different carboxylate oxygen atoms with a water molecule: C13–O15a···H–Ow1 and C13–O14···H–Ow1.

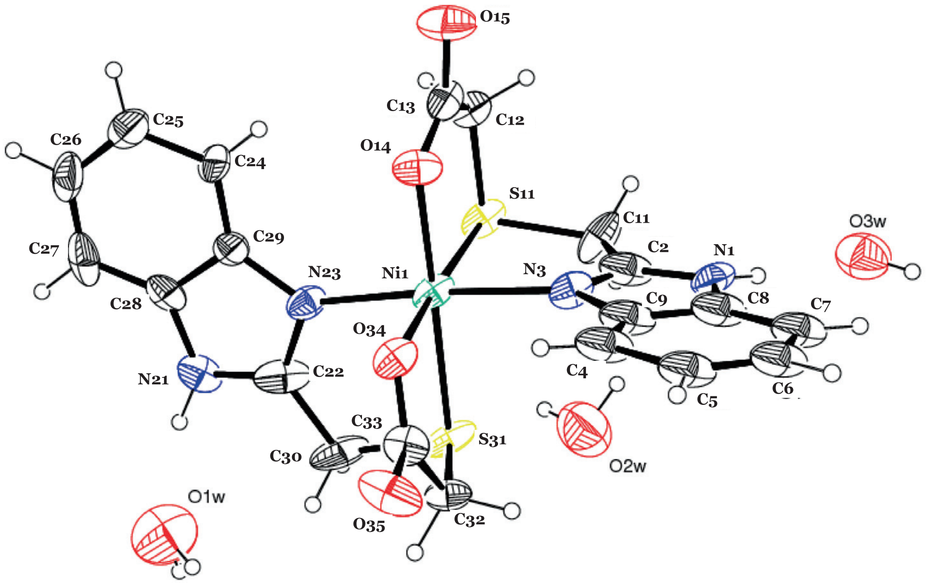

Fig. 4. ORTEP diagram of compound [Ni(bztb)$_2$]·3H$_2$O **2**. (Displacement ellipsoids are drawn at 30% probability).

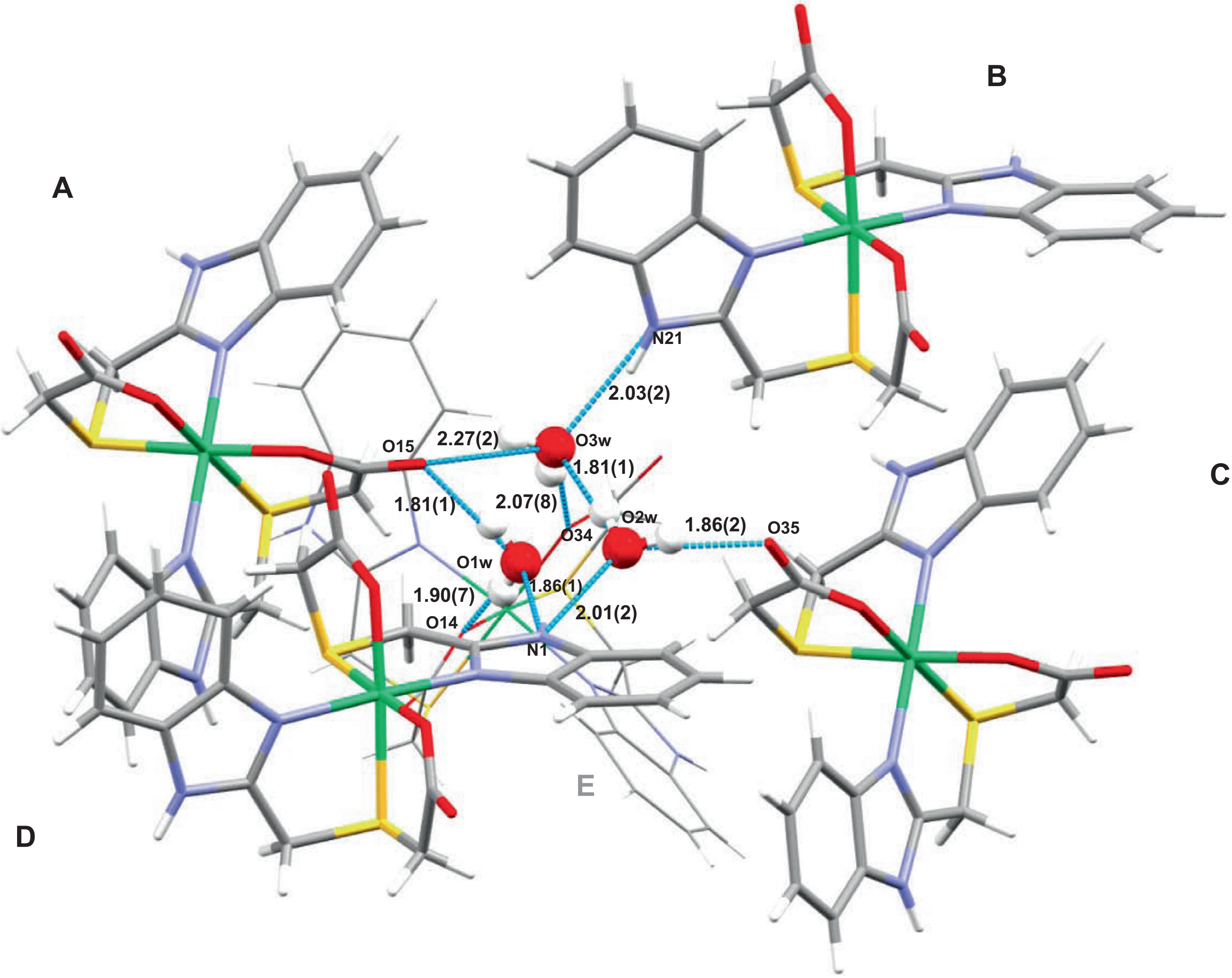

Fig. 5. Hydrogen bonding (Å) between the three uncoordinated water molecules and five [Ni(bztb)$_2$]·molecules.

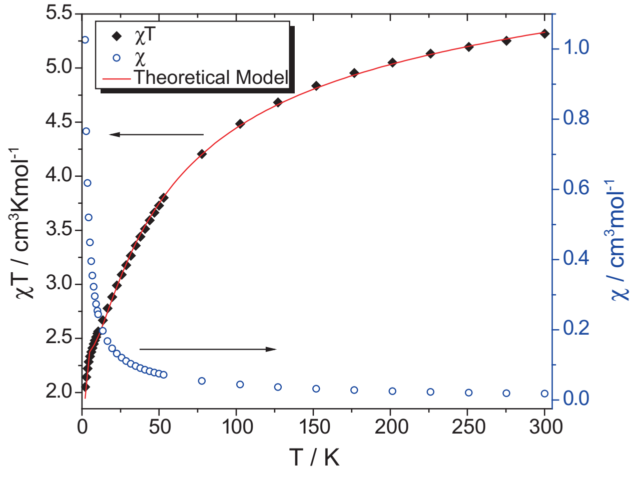

Fig. 6. Temperature dependence of $\chi_M T$ (♦) and χ_M (o) for the cobalt(II) compound **1**.

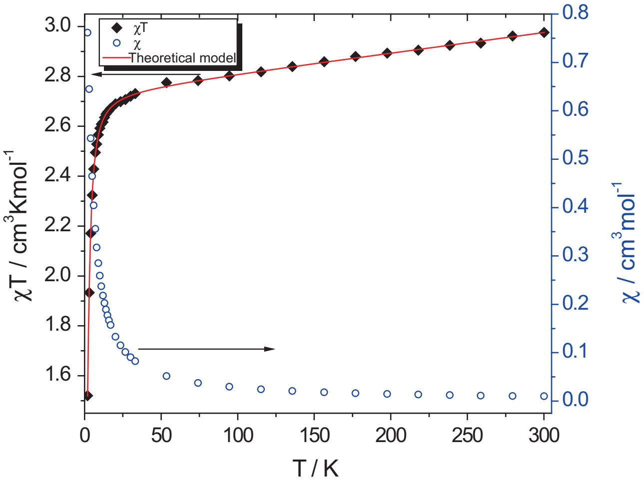

Fig. 7. Temperature dependence of $\chi_M T$ (♦) and χ_M (o) for the nickel(II) compound **2**.

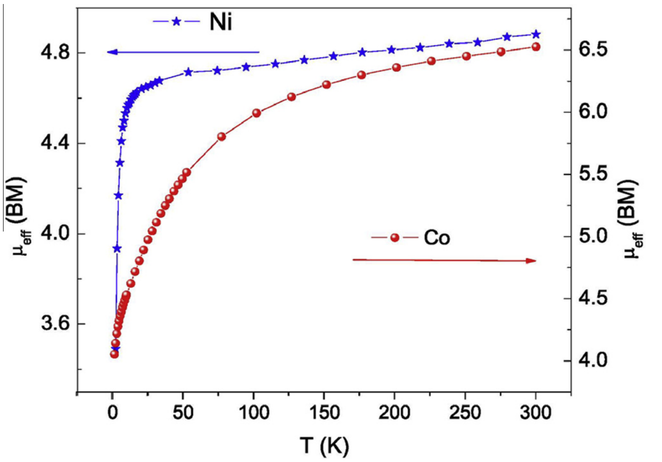

Fig. 8. Effective magnetic moment (μ_{eff}) of compound **1**(●) and **2** (★).

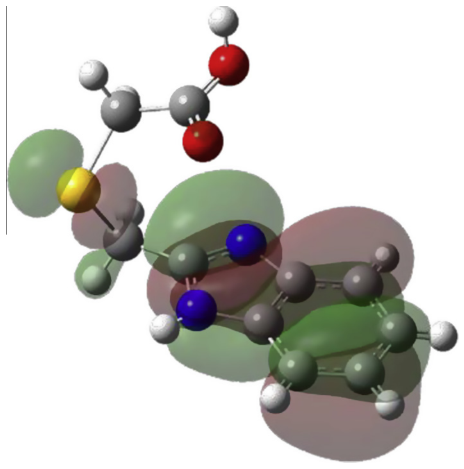

Fig. 9. Contour plot of the MO of the neutral Hbztb molecule.

with $D_2^2(5)$, $C_4^4(16)$, $R_4^4(32)$ and $R_6^6(48)$ motifs. Additionally, the 3D arrangement is further stabilized by intermolecular π–π stacking interactions between benzimidazolic rings as shown in Fig. 3, with a π–π stacking distance of 3.622 Å.

3.2.2. Compound [Ni(bztb)$_2$]·3H$_2$O (**2**)

Compound **2** consists of two deprotonated 4-(benzimidazol-2-yl)-3-thiabutanoic ligand (*bztb*) tricoordinated to the nickel(II) ion, stabilizing a *fac*-octahedral geometry, Fig. 4. In this structure the benzimidazolic nitrogen atoms are in a *trans* position, while the coordinated oxygen and sulfur donor atoms are in a *cis* arrangement, *fac*-Δ*S, S*, N-*trans*, which is a different isomer to the reported nickel(II) compound, in an all-*cis* arrangement[49]. The oxygen and sulfur donor atoms of the *bztb* form a square planar plane (O14, S11, S31, O34) around the central nickel(II), with a slight distortion of 0.0341 Å. Distances for the equatorial plane are approximately of 2.020 and 2.425 Å for Ni–O and Ni–S respectively (Table 2). As expected, the bond angles O14–Ni1–S11, O14–Ni1–O34, S11–Ni1–S31 show deviations from the orthogonality (Table 2). The axial positions are occupied by the nitrogen atoms, Ni–N (2.064(7) and 2.099(7) Å), Fig. 4, and Table 2. The angle S–M–S between the *cis*-S atoms is of 95.46°(8), whereas O–M–O, *cis*-O, is 94.60°(2) and for the *trans* N–M–N is 172.10°(3).

Note that the space group $P3_1$ corresponds to a chiral group, thus the nickel(II) compound **2** is an optical isomer [57], the Flack's parameter indicates that it is only one isomer present in this crystal, with an absolute configuration Δ. The reported analogue nickel(II) compound is the *cis* isomer, with a spatial group P_{21}/n, which is not chiral [49].

The three water molecules are in a triangular arrangement, as depicted in Fig. 5. The neutral complex and the water molecules establish multiple hydrogen bond interactions Ow–H···O and N–H···Ow, Table 3. There is a bifurcated hydrogen bond between N1–H and the oxygen atoms from the water molecules Ow1 and

Table 4
Magnetic and structural parameters for compounds **1** and **2**.

	μ_{eff}. [BM]	g_{iso}	D_{Mag}.[cm^{-1}]	E_{Mag}.[cm^{-1}]	D_{Str}.[cm^{-1}]	E_{Str}.[cm^{-1}]	$\chi_{TIP}/10^9$ [m^3 mol^{-1}]
[Co(Hbztb)$_2$]·2H$_2$O	6.52	2.0438	64.5	5.8	15.6	1.6	+9.35
[Ni(Hbztb)$_2$]·3H$_2$O	4.82	1.7654	2.7	1.2	2.5	0.8	+8.13

Ow2. Additionally, protons from Ow1–H, and Ow3–H are interacting with the carboxylate oxygen O15. In general, the water molecules provide a link between the metal compounds by a three-dimensional hydrogen bonding network, involving the water molecules (as donors and, in one case, as acceptor), the coordinated and uncoordinated oxygen of each carboxyl (as acceptors), and the benzimidazole N-H groups (as donors). Geometrical details of the hydrogen bonds are given in Table 3.

3.3. Magnetic characterization

An EPR study of the ligand Hbztb and its cobalt(II) coordination compound was undertaken at room temperature. It was observed that the ligand stabilizes a free radical with a $g = 1.9156$ with a coupling constant $A = 15.35$ Gauss, which indicates that the free radical is situated on a nitrogen atom; although its concentration is less than 2%. For the cobalt(II) compound, two signals were observed, $g_{||} = 2.731$ and $g_{\perp} = 2.129$, as it is expected for a cobalt(II) in an octahedral environment [58]. Additionally, a low intensity signal, $g = 2.0035$, was assigned to the free radical. It was found that its concentration was below 0.5%, so it is considered as a magnetic impurity.

Temperature dependent magnetic susceptibility measurements for the compounds **1** and **2** were performed on polycrystalline samples from 2 to 300 K. In both cases the susceptibility measurements, χ_M, were corrected for diamagnetism with the Pascal constants.

In Figs. 6 and 7 it is presented the susceptibility χ_M, and the product $\chi_M T$ as a function of temperature for both compounds. In the SI (Fig. SI-1) the values of the Curie constant, C, and Curie–Weiss temperature, obtained after fitting the inverse of the susceptibility (100–300 K), are included; $C = 5.83\ \text{cm}^3\ \text{mol}^{-1}$ K, and $\theta_{CW} = -30$ K. This value of C corresponds to a total spin, $s = 5/2$, where the spin–orbital contribution was taken into account. The obtained values, are consistent with a dinuclear cobalt(II) compound. In Table 4 it is shown selected data of the magnetic and structural parameters.

The magnetic data were fitted to the model for dinuclear cobalt(II) interaction through a modify Van Vleck equation [59], in which were included: the single-ion anisotropy and a paramagnetic impurity of the ligand free radical, the cobalt(II) spin–orbit contribution and the intermolecular interactions. The total spin $s = 5/2$, indicated that the coordination compound is behaving as a dimer, through intermolecular hydrogen bonding.

For the nickel(II) compound **2**, the Curie constant and the Curie–Weiss temperature, obtained after fitting the inverse of the susceptibility from 100 to 300 K, are the following: $C = 2.976\ \text{cm}^3\ \text{mol}^{-1}$ K and $\theta_{CW} = -4.5$ K, which correspond to a total spin of $s = 2$. Thus, the removal of the spin degeneracy will be $m_s = 0$ and $m_s = \pm 1$. The $\chi_M T$ observed at 300 K is $2.976\ \text{cm}^3\ \text{mol}^{-1}$ K [4,10,60–64]. This experimental data showed that the nickel(II) compound presents a dinuclear association, similar to the cobalt(II) compound **1** (Table 4).

M–H curves were measured at different temperatures for the Hbztb ligand and for compounds **1** and **2**, at magnetic fields from 0 to 2 T, these figures are included in the SI. The observed temperature behavior, for the ligand and the two coordination compounds, is in accord with the Brillouin model. The isothermal magnetization curves were measured at 2, 10 and 50 K. For the ligand, it corresponds to a value of $s = ½$. Both coordination compounds are weakly antiferromagnetic and the M–H isothermal measurements show weak ferromagnetism, indicative of canted spins. In both complexes the magnetic couplings may be a consequence of hydrogen-bonding.

The effective magnetic moment (μ_{eff}) values for the two compounds are displayed in Fig. 8. In the nickel(II) compound **2**, μ_{eff} is close to 4.8 BM at room temperature. Whereas for the cobalt(II) compound **1**, was not possible to define a clear value of μ_{eff}, how-

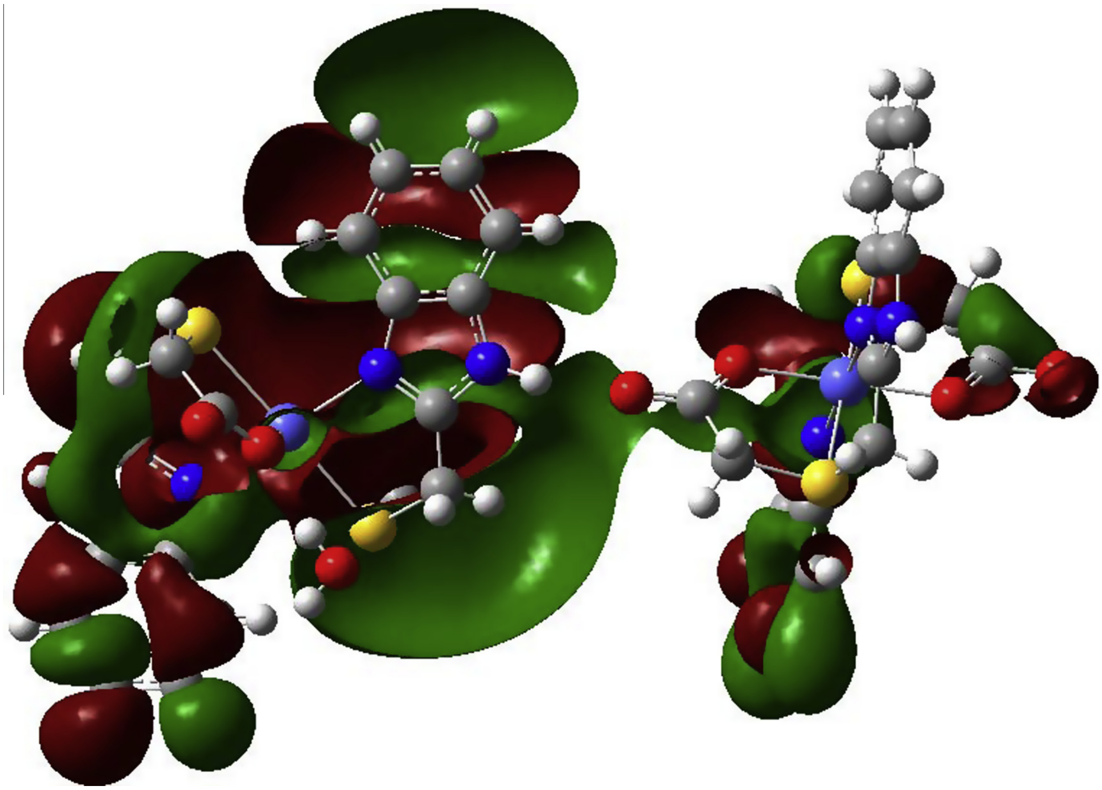

Fig. 10. Contour plot for the MO coupling the metal centers of the dinuclear [Co(bztb)$_2$···Co(bztb)$_2$] system; a threshold of ±0.001 a.u. was used.

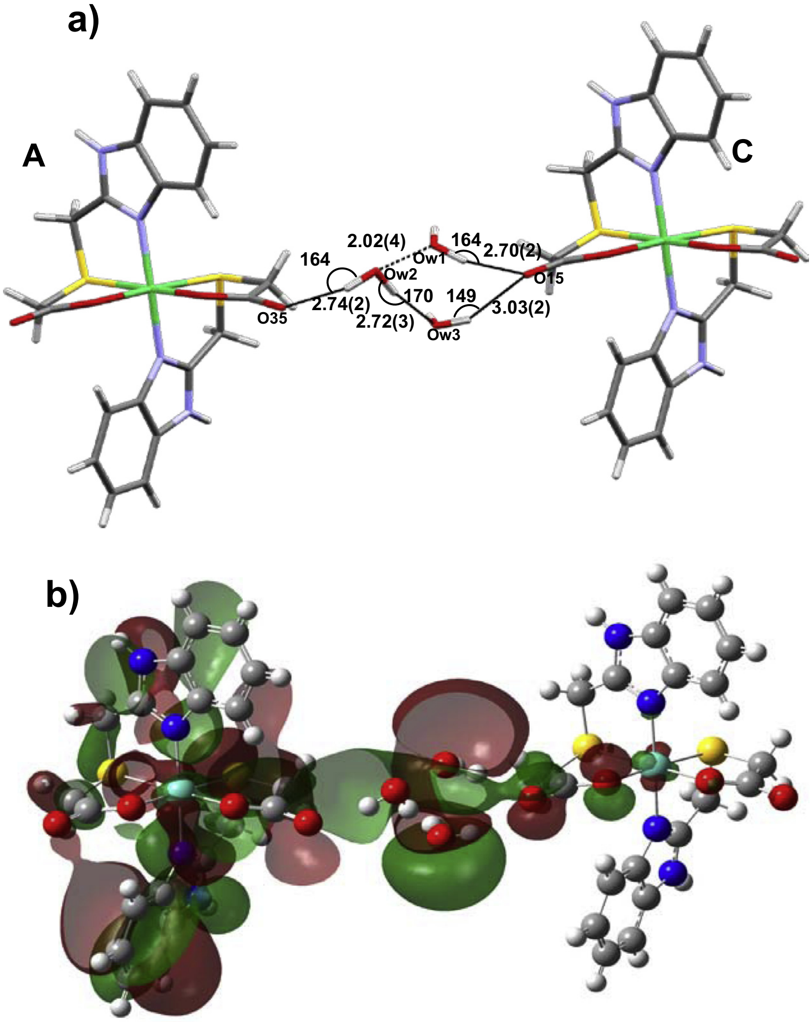

Fig. 11. Internuclear distances (Å) and angles (°) for: (a) non covalent interaction on the di-nuclear $[(Ni(bztb)_2\cdots(H_2O)_3\cdots Ni(bztb)_2]$ system; (b) Contour plot for the MO mainly contributing to the coupling of the metal centers; a threshold of ± 0.001 a.u. was used.

ever the effective magnetic moment at room temperature is close to 6.5 BM. These room temperature values corroborate the association of the monomers to give a dinuclear interaction, the data reported in the literature for cobalt(II) or nickel(II) dinuclear coordination compounds are similar [65–73]. On the other hand, it is important to discuss the different behavior of the μ_{eff} at low temperature for both compounds: whereas the nickel(II) shows a steep decrease of μ_{eff} below *ca.* 30 K; which is the signature of the zero field splitting of the energy levels, D, due to different interacting processes [60,74–77]; while for the cobalt(II) compound the decrease of μ_{eff} is almost constant, from high to low temperature. These two different behaviors are clearly due to the values of the total spin, and to the magnitude of the zero field splitting; in the cobalt(II) compound the splitting is given by $m_s = \pm 1/2$, and $m_s = \pm 3/2$ [60,75–77].

3.4. Theoretical ab initio study

To evaluate the contribution of the intermolecular interactions on the antiferromagnetic properties presented by these mononuclear compounds **1** and **2**, a Density Functional Theory (DFT) study was performed. Using the quantum chemistry software GAUSSIAN-09 [78], all-electron calculations were done at the B3LYP/6–311 + G(d,p) level of theory [79–84].

3.4.1. Ligand Hbztb

DFT calculations were realized in order to understand the electronic properties of the ligand and its complexes. The highest occupied molecular orbital (HOMO) of the Hbztb molecule (Fig. 9), presents important contributions on the region defined by the heteroatoms (N and S). As expected, the ligand coordinates through these atoms with the metal. Moreover, the estimated ionization energy (IE) of Hbztb, 7.85 eV, is relatively low, about half the IE of the hydrogen atom.

3.4.2. $2[Co(bztb)_2]\cdot 2H_2O$ (**1**)

The X-ray crystal structure of compound **1** reveals the presence of three different inter-molecular interactions: π-stacking between neighboring benzimidazole rings, hydrogen bonding of an imidazolic nitrogen with a carboxylate group N1–H···O15–C, hydrogen bonding of two carboxylates with a water molecule: C13–O14···H–Ow1 and C13–O15a···H-Ow1, as shown in Fig. 3. The possible contribution for each of these weak interactions to the magnetic coupling was studied.

For the isolated mononuclear cobalt(II) compound **1**, a quadruplet multiplicity was found as the most stable energy state. While for the dinuclear $[Co(bztb)_2\cdots Co(bztb)_2]$ system the quintuplet state was the one of lowest energy. Negligible contributions were found for π-stacking or hydrogen bonding (between the two protons of a water moiety and two carboxylates) to the magnetic coupling. The total energy difference between the di-nuclear $[Co(bztb)_2\cdots Co(bztb)_2]$ system and two monomeric species, indicates a binding energy of -14 kcal/mol for the di-nuclear system. That is, DFT calculations yield this value for the imidazolic N1–H···O14–C13 hydrogen bonding, which is mainly responsible for the attractive interaction of the monomers. Moreover, the N1–H···O14–C13 distance (2.07 Å) and the N1–H···O14 angle (167.25°) are consistent with such strong hydrogen bonding. The contour plot for the molecular orbital principally contributing to the coupling of the two monomeric moieties is depicted in Fig. 10. Note that the hydrogen atom of the bztb ligand is clearly polarized through the intermolecular N1–H···O14-C13 sigma bonds. Magnetic interaction has previously been proposed to be dependent on the orbital overlap [67–68,71–72], associated to the strength of the hydrogen bonds.

3.4.3. $[Ni(bztb)_2]\cdot 3H_2O$ (2)

In the crystal packing of compound **2**, there are relevant non-covalent interaction which contribute to the observed magnetic behavior. In Fig. 11a it is depicted the nickel(II) complexes A and C, the triangular arrangement of the water molecules and the intermolecular interactions that may contribute to the magnetic coupling between the two nickel(II) atoms. It is shown the directional character and distances of the hydrogen bonding between the three water molecules W1, W2 and W3 with the mononuclear complexes A and C, giving place to a dinuclear system. A triplet state was found as the one of lowest energy for the $[(Ni(bztb)_2\cdots(H_2O)_3\cdots Ni(bztb)_2]$.

In Fig 11b is shown the MO for the dinuclear $[(Ni(bztb)_2\cdots(H_2O)_3\cdots Ni(bztb)_2]$ system. The carboxylic group is coupled with the water molecules, through hydrogen bonding interactions. Which are mainly responsible for the super–exchange interaction in this di-nuclear association [69–70,73–74].

4. Conclusions

In conclusion, the 4-(benzimidazol-2-yl)-3-thiabutanoic acid (bztb), behaves as a tridentate ligand which may stabilized different octahedral isomers. $[Co(bztb)_2]\cdot 2H_2O$ **1**, is an all-trans isomer, while $[Ni(bztb)_2]\cdot 3H_2O$ **2**, stabilizes a fac-Δ *cis-cis–trans*-N compound. At low temperature, compounds **1** and **2** present weak antiferromagnetic couplings via intermolecular interactions. DFT calculations showed that in compound **1**, the hydrogen bonding between the benzimidazolic nitrogen and the neighboring carboxylic oxygen atom, contributes to the magnetic pathway for the coupling between the cobalt(II) complexes, which can be seen as a dinuclear $[Co(bztb)_2\cdots Co(bztb)_2]$ system, whereas the water molecules do not contribute to the magnetic behavior. On the other hand, calculations of compound **2**, indicated that two nickel(II) mononuclear compounds are linked by non-covalent interactions though three water molecules, $[(Ni(bztb)_2\cdots(H_2O)_3\cdots Ni(bztb)_2]$, which play an important role on the super-exchange magnetic coupling.

Acknowledgements

F. Yoe thanks to CONACyT for a scholarship. Also is acknowledge financial support to DGAPA UNAM, project IN222713, and CONACYT CB-2012 178851. RE, thanks partial support to CONACyT Project 129293 (Ciencia Básica), DGAPA-UNAM project IN100711, project BISNANO 2011, and project PICCO 11-7, by Institute of Sciences del Distrito Federal, Ciudad de Mexico.

Appendix A. Supplementary data

CCDC 921340 and 921341 contain the supplementary crystallographic data for compounds **1 and 2**, respectively. These data can be obtained free of charge from The Cambridge Crystallographic Data Centre via http://www.ccdc.cam.ac.uk/data_request/cif. Supplementary data associated with this article can be found, in the online version, at http://dx.doi.org/10.1016/j.ica.2014.07.025.

References

[1] Y. Wei, H. Hou, Y. Fan, Y. Zhu, Eur. J. Inorg. Chem. 19 (2004) 3946.
[2] C.G. Efthymiou, A.A. Kitos, C.P. Raptopoulou, S.P. Perlepes, A. Escuer, C. Papatriantafyllopoulou, Polyhedron 28 (2009) 3177.
[3] K. Hallier, M. Hołyńska, M. Rouzières, R. Clérac, S. Dehnen, Inorg. Chem. 51 (2012) 3929.
[4] G. Ambrosi, M. Formica, V. Fusi, L. Giorgi, M. Micheloni, Coord. Chem. Rev. 252 (2008) 1121.
[5] J. Klingele, S. Dechert, F. Meyer, Coord. Chem. Rev. 253 (2009) 2698.
[6] Yu.E. Alexeev, B.I. Kharisov, T.C. Hernández García, A.D. Garnovskii, Coord. Chem. Rev. 254 (2010) 794.
[7] S. Wang, X.-H. Ding, Y.-H. Li, W. Huang, Coord. Chem. Rev. 256 (2012) 439.
[8] S. Tanase, M. van Son, G.A. van Albada, R. de Gelder, E. Bowman, J. Reedijk, Polyhedron 25 (2006) 2967.
[9] M. Gembicky, R. Boča, L. Jäger, C. Wagner, Chem. Comm. 3 (2000) 566.
[10] D. Luneau, P. Rey, Coord. Chem. Rev. 249 (2005) 2591.
[11] A.I. Poddel'sky, V.K. Cherkasov, G.A. Abakumov, Coord. Chem. Rev. 253 (2009) 291.
[12] F.-H. Zhao, Y.-X. Che, J.-M. Zheng, F. Grandjean, G.J. Long, Inorg. Chem. 51 (2012) 4862.
[13] C. Yang, M.Y. Tsai, S.-W. Hung, J.-H. Chen, S.-S. Wang, J.-Y. Tung, Polyhedron 37 (2012) 1.
[14] P. Gütlich, A.B. Gaspar, V. Ksenofontov, Y. Garcia, J. Phys. Condens. Matter 16 (2004) S1087.
[15] B. Dojer, A. Pevec, P. Šegedin, Z. Jagličić, C. Stropnik, Inorg. Chim. Acta 363 (2010) 1343.
[16] A. Buchholz, A.O. Eseola, W. Plass, C. R. Chimie 15 (2012) 929.
[17] X. Shan, A.O. Ibrahim, Y. Zhou, H. Zhang, J. Ma, F. Jiang, M. Hong, Inorg. Chem. Commun. 22 (2012) 149.
[18] K. Helios, M. Duczmal, A. Pietraszko, D. Michalska, Polyhedron 49 (2013) 259.
[19] T. Miyake, T. Ishida, D. Hashizume, F. Iwasaki, T. Nogami, Polyhedron 20 (2001) 1551.
[20] A. Mašlejová, R. Boča, Ľ. Dlháň, B. Papánková, I. Svoboda, H. Fuess, Chem. Phys. Lett. 347 (2001) 397.
[21] B. Dojer, A. Pevec, P. Šegedin, Z. Jagličić, Č. Stropnik, M. Kristl, M. Drofenik, Inorg. Chim. Acta 363 (2010) 1343.
[22] B. Papánková, R. Boča, Ľ. Dlháň, I. Nemec, J. Titiš, I. Svoboda, H. Fuess, Inorg. Chim. Acta 363 (2010) 147.
[23] F.-H. Zhao, Y.-X. Che, J.-M. Zheng, Inorg. Chem. 51 (2012) 4862.
[24] W.A. Skinnerm, M.G.M. Schelstraete, B.R. Baker, J. Org. Chem. 24 (1959) 1827.
[25] K.K. Biron, Antiviral Res. 71 (2006) 154.
[26] T. Middleton, H.B. Lim, D. Montgomery, T. Rockway, H. Tang, X. Cheng, L. Lu, H. Mo, W.E. Kohlbrenner, A. Molla, W.M. Kati, Antiviral Res. 64 (2004) 35.
[27] L. Labanauskas, A. Brukštus, E. Udrėnaitė, P. Gaidelis, V. Bučinskaitė, Chemija (Vilnius) 14 (2003) 49.
[28] H. Sari, A.K. Covington, J. Chem. Eng. Data 50 (2005) 1425.
[29] M. Meaney, J. Allister, B. McKinstry, K. McLaughlin, G.P. Brennan, A.B. Forbes, I. Fairweather, Parasitol. Res. 100 (2007) 1091.
[30] A.N. Mirskova, G.G. Levkovskaya, R.G. Mirskov, M.G. Voronkov, Russ. J. Org. Chem. 44 (2008) 1478.
[31] Y. Miyazaki, T. Sakakibara, J.R. Ferrer, P.M. Lahti, G. Antorrena, F. Palacio, M. Sorai, J. Phys. Chem. B 106 (2002) 8615.
[32] Y. Miyazaki, A. Inaba, S. Michio, P.S. Taylor, P.M. Lahti, J. Phys. Chem. B 112 (2008) 8144.
[33] J. Kabatc, K. Jurek, Polymer 53 (2012) 1973.
[34] Y. Elerman, I. Svoboda, Acta Cryst. C52 (1996) 2705.
[35] T. Tsotakos, C. Tsoukalas, G. Patsis, A. Panagiotopoulou, N. Nikolić, D. Janković, D. Djokić, C.P. Raptopoulou, A. Terzis, D. Papagiannopoulou, M. Pelecanou, M. Papadopoulos, I. Pirmettis, Inorg. Chim. Acta 377 (2011) 62.
[36] T. Yonemura, T. Yasui, K.-I. Okamoto, J. Hidaka, Acta Cryst. C 52 (1996) 1390.
[37] A.P. Gulea, S.N. Spynu, V.I. Tsapkov, D. Poirier, J. Roy, Russ. J. Gen. Chem. 76 (2006) 1458.
[38] P.K. Mascharak, Coord. Chem. Rev. 225 (2002) 201.
[39] E. Bouwman, J. Reedijk, Coord. Chem. Rev. 249 (2005) 1555.
[40] V.E. Kaasjager, L. Puglisi, E. Bouwman, W.L. Driessen, J. Reedijk, Inorg. Chim. Acta 310 (2000) 183.
[41] L. Gomes, E. Pereira, B. de Castro, J. Chem. Soc., Dalton Trans. 8 (2000) 1373.
[42] P.R. Reddy, K.S. Rao, B. Satyanarayana, Tetrahedron Lett. 47 (2006) 7311.
[43] P.R. Reddy, N. Rajuo, K.S. Rao, A. Shilpa, India J. Chem. 48A (2009) 761.
[44] S.A. Patil, V.H. Naik, A.D. Kulkarni, P.S. Badami, Spectrochim. Acta 75A (2010) 347.
[45] Y.-L. Wong, A.R. Cowley, J.R. Dilworth, Inorg. Chim. Acta 357 (2004) 4358.
[46] M.U. Raja, N. Gowri, R. Ramesh, Polyhedron 29 (2010) 1175.

[47] H. He, M. Lipowska, X. Xu, A.T. Taylor, M. Carlone, L.G. Marzilli, Inorg. Chem. 44 (2005) 5437.

[48] M. Saadeh, H.M.A. Shawish, H.M. Dalloul, N.M. EL-Halabi, B.Kh. Daher, Mater. Sci. Eng. C 32 (2012) 619.

[49] C.J. Matthews, S.L. Heath, M.R.J. Elsegood, W. Clegg, T.A. Leese, J.C. Lockhart, J. Chem. Soc., Dalton Trans. 12 (1998) 1973.

[50] B.B. Mahapatra, S. Ku, Biokemistri 22 (2010) 71.

[51] Oxford Diffraction. CrysAlis CCD and CrysAlis RED. Oxford Diffraction Ltd, Abingdon, England, 2007.

[52] R.C. Clark, J.S. Reid, Acta Cryst. A 51 (1995) 887.

[53] G.M. Sheldrick, SHELXS97 and SHELXL97, University of Gottingen, Germany, 2008.

[54] L.J. Farrugia, J. Appl. Cryst. 30 (1997) 565.

[55] L.J. Farrugia, J. Appl. Cryst. 32 (1999) 837.

[56] E. Bouwman, J. Reedijk, Inorg. Chim. Acta 215 (1994) 151.

[57] A. Mohamadou, K. Ple, A. Haudrechy, Chem. Edu. 88 (2011) 302.

[58] R.S. Drago. Physical Methods for Chemists, second ed., Saunders College Pub., 1992.

[59] F. Lloret, M. Julve, J. Cano, R. Ruiz-García, E. Pardo, Inorg. Chim. Acta 361 (2008) 3432.

[60] P. Baran, M. Boca, R. Boca, A. Krutosikova, J. Miklovic, J. Pelikan, J. Titis, Polyhedron 24 (2005) 1510.

[61] A. Kubica, J. Kowaleski, D. Kruk, M. Odelius, J. Chem. Phys. 138 (2013) 064304.

[62] R. Ivanikova, R. Boca, L. Dlhan, H. Fuess, A. Maslejova, V. Mrazova, I. Svoboda, J. Titis, Polyhedron 25 (2006) 3261.

[63] R. Ranjan, R. Rani, S. Suman Singh, A.K. Singh, S. Sharma, Asian J. Chem. 22 (2010) 7580.

[64] P. Bhowmik, S. Chattopadhyay, M.G.B. Drew, C. Diaz, A. Ghosh, Polyhedron 29 (2010) 2637.

[65] F. Isik, M.A. Sabaner, S. Gürler, A. Bayri, J. Supercond. Nov. Mag. 24 (2011) 641.

[66] M. Idešicová, A. Krutošíková, V. Mrázová, R. Boča, Chem. Pap. 67 (2013) 300.

[67] S. Tanase, M. Van Son, G.A. Van Albada, R. de Gelder, E. Bouwman, J. Reedijk, Polyhedron 25 (2006) 2967.

[68] J. Titiš, J. Hudák, J. Kozíšek, A. Krutošíková, J. Moncol', D. Tarabová, R. Boča, Inorg. Chim. Acta 388 (2012) 106.

[69] R. Ivaniková, R. Boča, L. Dlháň, H. Fuess, A. Mašlejová, V. Mrázová, I. Svoboda, J. Titiš, Polyhedron 25 (2006) 3261.

[70] J. Titiš, R. Boča, L'. Dlháň, T. Ďurčeková, H. Fuess, R. Ivaniková, V. Mrázová, B. Papánková, I. Svoboda, Polyhedron 26 (2007) 1523.

[71] R. Herchel, R. Boča, Dalton Trans. 8 (2005) 1352.

[72] A. Okazawa, T. Ishida, Chem. Phys. Lett. 480 (2009) 198.

[73] N. Pan, R.-Z. Wei, Y.-H. Chi, J.-M. Shi, W. Wei, Y.-Q. Zhang, Z. Anorg. Allg. Chem. 639 (2013) 1026.

[74] A. Maslejova, R. Ivanikova, I. Svoboda, B. Papankova, L. Dlhan, D. Miklos, H. Fuess, R. Boca, Polyhedron 25 (2006) 1823.

[75] J. Titis, R. Boca, L. Dlhan, T. Durcekova, H. Fuess, R. Ivanikova, V. Mrazova, B. Papankova, I. Svoboda, Polyhedron 29 (2007) 1523.

[76] M. Sebova, V. Jorik, J. Moncol, J. Kozisek, R. Boca, Polyhedron 30 (2011) 1163.

[77] J. Titis, R. Boca, Inorg. Chem. 49 (2010) 3971.

[78] Gaussian 09, Revision D.01, M.J. Frisch, G.W. Trucks, H.B. Schlegel, G.E. Scuseria, M.A. Robb, J.R. Cheeseman, G. Scalmani, V. Barone, B. Mennucci, G.A. Petersson, H. Nakatsuji, M. Caricato, X. Li, H.P. Hratchian, A.F. Izmaylov, J. Bloino, G. Zheng, J.L. Sonnenberg, M. Hada, M. Ehara, K. Toyota, R. Fukuda, J. Hasegawa, M. Ishida, T. Nakajima, Y. Honda, O. Kitao, H. Nakai, T. Vreven, J.A. Montgomery, Jr., J.E. Peralta, F. Ogliaro, M. Bearpark, J.J. Heyd, E. Brothers, K.N. Kudin, V.N. Staroverov, T. Keith, R. Kobayashi, J. Normand, K. Raghavachari, A. Rendell, J.C. Burant, S.S. Iyengar, J. Tomasi, M. Cossi, N. Rega, J.M. Millam, M. Klene, J.E. Knox, J.B. Cross, V. Bakken, C. Adamo, J. Jaramillo, R. Gomperts, R.E. Stratmann, O. Yazyev, A.J. Austin, R. Cammi, C. Pomelli, J.W. Ochterski, R.L. Martin, K. Morokuma, V.G. Zakrzewski, G.A. Voth, P. Salvador, J.J. Dannenberg, S. Dapprich, A.D. Daniels, O. Farkas, J.B. Foresman, J.V. Ortiz, J. Cioslowski, D.J. Fox, Gaussian, Inc., Wallingford CT, 2013.

[79] A.D. Becke, J. Chem. Phys. 98 (1993) 5648.

[80] C. Lee, W. Yang, R.G. Parr, Phys. Rev. B 37 (1988) 785.

[81] B. Miehlich, A. Savin, H. Stoll, H. Preuss, Chem. Phys. Lett. 157 (1989) 200.

[82] K. Raghavachari, G.W. Trucks, J. Chem. Phys. 91 (1989) 1062.

[83] T. Clark, J. Chandrasekhar, G.W. Spitznagel, P.V.R. Schleyer, J. Comput. Chem. 4 (1983) 294.

[84] A.H. Pakiari, K. Eskandari, J. Mol. Struct. Theochem. 759 (2006) 51.